Microchim Acta (2016) 183:917–921
DOI 10.1007/s00604-015-1704-4

SHORT COMMUNICATION

Silver nanoparticle induced chemiluminescence of the hexacyanoferrate-fluorescein system, and its application to the determination of catechol

Suqin Han[1] · **Bibi Liu**[1] · **Yan Liu**[1] · **Zheyan Fan**[1]

Received: 10 October 2015 / Accepted: 2 December 2015 / Published online: 14 December 2015

Abstract The article describes a flow injection chemiluminescence (CL) assay for catechol. It is based on the catechol-induced reduction of the CL of a system composed of fluorescein, hexacyanoferrate(III) and silver nanoparticles in strongly alkaline solution. Under the selected conditions, the decrease in CL intensity is proportional to the concentration of catechol in the 0.1 to 10 μM range. The detection limit is 5.0 nM, and the relative standard deviation is 1.5 % (for $n = 11$ at a 1.0 μM concentration of catechol). The method was successfully applied to the determination of catechol in spiked environmental water samples.

Keywords Flow injection · Poly(vinyl pyrrolidone) · Environmental analysis · Water analysis · TEM

Introduction

Chemiluminescence (CL), a light emission induced by chemical reaction, has been intensively investigated for many years [1]. CL method has many advantages, such as simple equipment, high sensitivity and low background signals. The CL study has been extended to nanoparticles systems from traditional molecular systems among nanoparticles as a catalyst, reductant, luminophor, and energy acceptor [2, 3]. In particular, silver nanoparticles (AgNPs) have a redox potential lower than that of gold, platinum and so on. AgNPs have been used in the luminol [4, 5], bis (2,4, 6-tricholorophenyl) oxalate [6, 7], Ce(IV) [8] and $KMnO_4$ [9] system.

Catechol is a natural polyphenolic compound which is ubiquitous in nature since it commonly generates in factory processes and widely exists in higher plants such as teas, fruits, tobaccos and some traditional Chinese medicines. It is widely used in the area of cosmetics, tanning, pesticides, medicines and photography chemicals [10]. Catechol is easily absorbed from the gastrointestinal tract, causing vasoconstriction, renal tube degeneration, liver function decrease, cancers and neurodegenerative diseases, besides accumulating in bone marrow [11]. So, catechol is extremely harmful to animals, plants and aquatic environments even at very low concentration, and is considered one of the environmental pollutants by the US Environmental Protection Agency [12]. Consequently, sensitive and rapid simultaneous determination of catechol is required. Several analytical methods have been used for the determination of catechol, such as spectrophotometry [13, 14], electrochemistry [15–20], electrogenerated CL [21, 22], gas chromatography [23], high-performance liquid chromatography [24] and capillary electrophoresis [25–27].

The study showed that AgNPs induces the CL of the $K_3Fe(CN)_6$-fluorescein system but that the CL intensity of $K_3Fe(CN)_6$-fluorescein-AgNPs is reduced in the present of catechol and the decrease CL intensity is proportional to the catechol concentration in a certain range. Hence, a CL method has been designed for the analysis of catechol in environment waters. The reaction mechanism is also discussed.

Electronic supplementary material The online version of this article (doi:10.1007/s00604-015-1704-4) contains supplementary material, which is available to authorized users.

✉ Suqin Han
hsq@dns.sxnu.edu.cn

[1] School of Chemistry and Material Science, Shanxi Normal University, Linfen 041004, Shanxi, People's Republic of China

Experimental

Apparatus

CL measurements were carried out on an IFIS-C intelligent flow injection sampler (Xi'an Remax Analytical Instrument Co. Ltd., Shannxi, China, http://www.chinaremex.com/) and BPCL-1-TIC ultra weak CL analyzer (Beijing Jianxin Lituo Company, Beijing, China, http://www.bpcl.com.cn/). CL spectra were measured with Cary Eclipse spectrofluorimeter (Varian, USA, http://varian.lookchem.com/). Absorption spectra were taken on a Cary5000 spectrophotometer (Varian, USA, http://varian.lookchem.com/). The centrifugal separation was carried out on the TGL-16G centrifuge (Shanghai Anting Scientific Instrument Factory, Shanghai, China, http://www.centrifuge.com.cn/).

Reagents

Catechol and silver nitrate were purchased from Tianjin Chemical Reagent Company (Tianjin, China, http://sjyc.company.lookchem.cn/). Poly(vinyl pyrrolidone) (the mean molecular weight is 10,000 g·moL^{-1}), fluorescein, sodium citrate, sodium borohydride and $K_3Fe(CN)_6$ were purchased from Sinopharm Group Chemical Reagent Co. Ltd. (Shanghai, China, http://www.reagent360.cnal.com/).

The 0.01 M stock solution of catechol and $K_3Fe(CN)_6$ were prepared in water, respectively. The 0.1 mM working solution of $K_3Fe(CN)_6$ was prepared by diluting the stock solution in 0.1 M NaOH. The 0.01 M stock solution of fluorescein was prepared by dissolving fluorescein in 0.1 M NaOH and diluting to 100 mL with water. The working solution of fluorescein was prepared by diluting the stock solution in water. All the reagents used were of analytical reagent grades and doubly distilled water was used throughout the whole experiment.

Preparation of AgNPs

AgNPs was synthesized by chemical reduction method according to the literature [28] with some modification. In brief, 0.30 g poly(vinyl pyrrolidone) was dissolved in 10.0 mL water and mixed with the 10.0 mL 0.02 M $AgNO_3$ solution. Then, 2.0 mL 0.1 M $NaBH_4$ was added dropwise to the mixture under vigorous stirring. The mixture color changed to yellow gradually. The reaction was conducted at room temperature for 30 min and aged for 2 days at 4 °C. The raw colloid was centrifuged at 10,376 rcf for 30 min. AgNPs were characterized by UV-vis spectrophotometer and the surface plasmon resonance band of AgNPs appears at 430 nm. Statistical analysis of the TEM image revealed that the average diameter of the AgNPs was about 50 nm ± 5 nm, which was calculated by 50 particles. (Fig. S1, Electronic Supplementary Material, ESM). The concentration of AgNPs was calculated by the number of silver atoms contained in the sample.

Procedure

The flow injection CL detection system employed in this work was described in Fig. 1. The carrier water, $K_3Fe(CN)_6$ solution, the mixed solution of fluorescein and AgNPs were continuously pumped at a flow rate of 3.6 mL·min^{-1} into the flow cell. The catechol standard or sample solution was injected by an eight-way injection valve with a sample loop of 100 μL. The CL signal produced in the flow CL cell was monitored by a photomultiplier tube (PMT, operated at −700 V) and was recorded by a computer equipped with a data acquisition interface. Data acquisition and treatment were performed with BPCL software running under Windows XP. The concentration of catechol was quantified by measuring the decrease CL intensity, $\Delta I = I_0 - I_s$, where I_0 and I_s were CL intensity in the absence and presence of catechol.

Results and discussion

Kinetic characteristic of CL reaction

The CL intensity-time curve is shown in Fig. S2 (ESM). No detectable CL emission can be recorded for $K_3Fe(CN)_6$-fluorescein system in the absence of AgNPs. When $K_3Fe(CN)_6$ solution was injected into the mixture solution of fluorescein and AgNPs, a strong CL reaction was initiated immediately and the maximum CL intensity was obtained in 0.5 s (peak a). Therefore, the CL emission was attributed to the catalytic effect of the AgNPs on the $K_3Fe(CN)_6$-fluorescein system. Further, a inhibitory CL signal occurred after the catechol was added to the $K_3Fe(CN)_6$-fluorescein-AgNPs system (peak b).

Optimization of the reaction conditions

A series of experiments were conducted to select the optimum analytical conditions using a 1.0 μM catechol solution. The optimized parameters included the concentration of $K_3Fe(CN)_6$, fluorescein, NaOH and AgNPs, the flow rate of reagents.

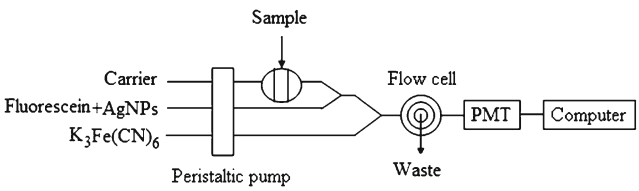

Fig. 1 Schematic diagram of the flow injection chemiluminescence system

The effect of $K_3Fe(CN)_6$ concentration on the CL reaction was examined in the range of 0.1–0.5 mM. The experiments showed the maximal CL signal is obtained when the concentration of $K_3Fe(CN)_6$ was 0.3 mM (Fig. S3A, ESM). The fluorescein concentration was studied in the range of 0.1–0.5 mM. As shown in Fig. S3B, ESM, the CL intensity increased with increasing the concentration of fluorescein. When the fluorescein concentration was in the range of 0.25–0.35 mM, the CL signal reached a maximum value, and then decreased above 0.35 mM. Therefore, the fluorescein concentration of 0.3 mM was selected for further studies. The effect of NaOH concentration from 0.06 to 0.14 M added in $K_3Fe(CN)_6$ solution was investigated (Fig. S3C, ESM). The CL intensity increased with the concentration of NaOH and reached the maximum at 0.1 M NaOH, then decreased. That might be due to the fact that the catalytic ability of AgNPs declined in the high alkaline media. Thus, 0.1 M NaOH was selected as the optimal concentration for further experiments. The AgNPs concentration was varied from 0.3 to 0.8 μM. The CL intensity increased steadily with AgNPs concentration and then decreased probably due to the strong interaction among the particles (Fig. S3D, ESM). It was found that when the concentration of AgNPs solution was 0.55 μM, CL signal reached the highest. Thus 0.55 μM was selected as optimum concentration.

The flow rate of reagents played an important role in CL measurements, as the time consumed to transfer the excited product into the flow cell is critical parameter for achieving maximum amount of the emitted light. Therefore, the flow rate was studied over the range 2.0–4.5 $mL \cdot min^{-1}$ with equal flows in each channel, while keeping all other conditions as constant. The results showed that the CL signal increased with the increasing of flow rate, then decreased. So, the flow rate of 3.6 $mL \cdot min^{-1}$ was selected under the present conditions.

Analytical performance

Under the optimum conditions, the relative CL intensity was linear to the concentration of catechol over the range 0.1 to 10.0 μM. The regression equation was $\Delta I = 261.8c + 69.24$ (where c was the concentration of catechol in 1.0 μM) with a correlation coefficient of 0.9994 (Fig. 2). The determination limit was 5.0 nM catechol (3σ). The relative standard deviation was 1.5 % by 11 replicate determinations of 1.0 μM catechol. These indicated that the CL method has good linearity, relatively high sensitivity and precision and acceptable reproducibility. Compared with most of the nanomaterial-based methods [15–19, 21], this method had lower detection limit (Table 1).

Interference

The influence of potential interferences was investigated by analyzing a standard solution of 1.0 μM catechol with varying amounts of interfering species. A substance was considered no interference if the variation of the CL intensity was within ±5 %. The tolerable concentration ratios of potentially interfering compounds to 1.0 μM catechol were over 3000-fold for NH_4^+, Zn^{2+}, Pb^{2+}, Al^{3+}, CO_3^{2-} and HCO_3^-; 1000-fold for K^+, NO_3^-, Na^+, SO_4^{2-}, Ca^{2+}, Mg^{2+} and Cl^-; 300-fold for Cu^{2+}, Mn^{2+}, ether, formic acid and alcohol; 100-fold for Fe^{3+}, Co^{2+} and benzoic acid; 50-fold for Hg^{2+}, Cd^{2+} and Fe^{2+}; 10-fold for ortho-hydroxybenzoic acid and phenol; 5-fold for resorcinol and hydroquinone.

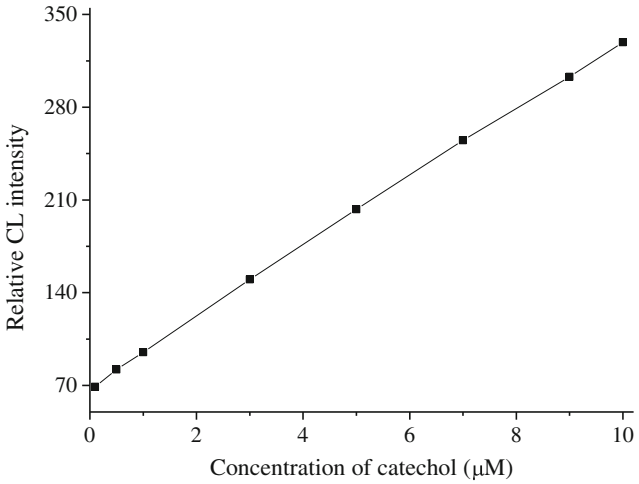

Fig. 2 Calibration plot for the determination of catechol

Analysis of tap water and lake water

The CL method has been applied to the determination of catechol in tap water and lake water. The results were given in Table 2. In order to evaluate the validity of the analysis method, these samples were prepared by adding the standard solution of catechol and were tested. The recovery experiments were carried out by adding a standard catechol solution to tap water and lake water. The recovery was range from 99 % to 105 %. The results confirmed the accuracy of the method.

Chemiluminescence mechanism

The CL spectra of $K_3Fe(CN)_6$-fluorescein system in the absence and presence of AgNPs was recorded and was shown in Fig. 3. Almost no CL signal was detected for the reaction between $K_3Fe(CN)_6$ and fluorescein. After adding AgNPs into the system a strong CL signal occurred (curve b). The maximum wavelength is 520 nm, which was in agreement with the fluorescent spectrum of fluorescein. This indicated that the CL emission was from the excited state of fluorescein, and AgNPs played an enhanced role in light emission. When catechol was added to the system, the CL intensity was markedly inhibited and the maximum wavelength was still 520 nm (curve a).

Table 1 Figures of merit of recently reported nanomaterial-based methods for determination of catechol

Materials/Method	Linear range (μM)	Detection limit (μM)	Matrix	Reference
Nanoporous gold/Electrochemistry (EC)	50–1000	1.78	—	15
Cobalt ferrite/EC	1–200	0.12	Water	16
Graphitic carbon nitride nanosheets-carbon nanotube composite/EC	1–200	0.09	Water	17
Nanopore array derived from l-cysteine oxide/gold hybrids/EC	0.8–500	0.034	Water	18
Gold nanoparticles/ZnS/NiS@ZnSQDs/EC	0.5–400	0.071	Water	19
Gold nanoparticles@C_{60}/electrogenerated CL	0.062–120	0.021	Water	21
AgNPs/CL	0.1–10.0	0.005	Water	This work

The UV-vis spectra were investigated. Fig. S4A showed that $K_3Fe(CN)_6$ showed two absorption peaks at about 300 nm and 420 nm (curve a), fluorescein showed a absorption peak at about 492 nm (curve b) and AgNPs showed a absorption peak at about 430 nm (curve d). The absorption value of the $K_3Fe(CN)_6$ and fluorescein mixed system almost equaled to the sum of two individual systems (curve c), which meant that no obvious reaction occurred. When AgNPs was added to the system, the characteristic absorption peak of hexacyanoferrate and fluorescein disappeared. The absorption peak of the $K_3Fe(CN)_6$-fluorescein-AgNPs system (curve e) occurred at 443 nm and the absorption intensity greatly enhanced. Therefore, it is presumed that the reaction take place between $K_3Fe(CN)_6$ and fluorescein in the presence of AgNPs. The characteristic absorption peak of catechol displayed at 276 nm (Fig. S4B). When $K_3Fe(CN)_6$ was mixed with catechol, the characteristic absorption peak of catechol disappeared.

The solutions of $K_3Fe(CN)_6$, fluorescein and AgNPs were saturated with O_2 and N_2 by bubbling and then the system was examined under saturated conditions. The CL intensity for saturated and normal conditions decreased in the order O_2 saturated > normal > N_2 saturated, suggesting the participation of O_2 in the course of the CL reaction.

Based on the above experiments and discussion, a possible CL reaction mechanism was as follows: under the catalytic action of AgNPs, a portion of fluorescein was oxidized by $K_3Fe(CN)_6$ accompanied by a release of energy and other fluorescein absorbed that energy and produced excited state fluorescein. The fluorescein of the excited state returned to the ground state, accompanied by CL. On the other hand, under the catalytic action of AgNPs, dissolved oxygen adsorbed on the surface of AgNPs formed superoxides. Superoxides were reacted with water to generate hydrogen peroxide [29]. The produced H_2O_2 was mixed with $K_3Fe(CN)_6$ in an alkaline medium to produce oxygen [30]. The produced superoxide radical reacted with the fluorescein to yield excited state fluorescein and the CL emission was produced when excited state fluorescein returned to the ground state. Catechol as a reducing agent was able to react with $K_3Fe(CN)_6$ and reduced the formation of excited state fluorescein, and then the CL emission was inhibited.

Table 2 The determination of catechol in tap and lake water (n = 11)

Samples	Added (μM)	Found (μM)	Recovery (%)	RSD (%)
Tap water	0	0.75	–	1.4
	2.0	2.85	105	1.9
	4.0	4.82	102	2.0
Lake water	0	0.82	–	2.5
	2.0	2.90	104	2.4
	4.0	4.79	99	2.2

Conclusion

AgNPs are found to enhance the weak CL of the $K_3Fe(CN)_6$-fluorescein system. Based on the inhibitory effect of catechol on the CL reaction in alkaline solution, a sensitive CL method was developed for the determination of catechol in tap and lake water samples with satisfactory results. The method is rapid and simple, in addition to high sensitivity, low detection limit and less interference. This work was important for the investigation of efficient catalysts for weak CL system and the comprehension of CL mechanism correspondingly. Further

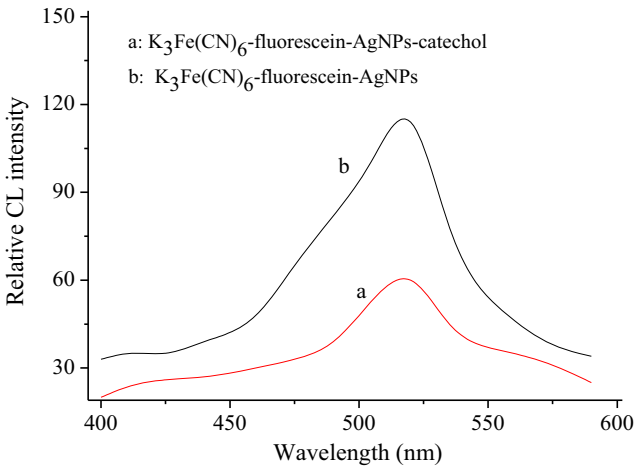

Fig. 3 Chemiluminescence spectra

investigation is necessary to decide whether the CL system can be suitable for other phenolic compounds and some drugs which contain phenolic hydroxy groups.

Acknowledgments This work was financially supported by the Natural Science Foundation of Shanxi (Grant No. 2013011013-3), Undergraduate Training Programs for Innovation and Entrepreneurship of Shanxi Normal University (SD2014CXXM-50 and SD2015CXXM-79) and Shanxi Normal University of Modern Arts and Sciences (WL2014CXCY-10). All the authors express their deep thanks.

References

1. Mervartová K, Polášek M, Calatayud JM (2007) Recent applications of flow injection and sequential-injection analysis techniques to chemiluminescence determination of pharmaceuticals. J Pharm Biomed Anal 45:367–381
2. Li Q, Zhang L, Li J, Lu C (2011) Nanomaterial-amplified chemiluminescence systems and their applications in bioassays. TrAC Trends Anal Chem 30:401–413
3. Chao Y, Zhang X, Liu L, Tian L, Pei M, Cao W (2015) Determination of hydroquinone by flow injection chemiluminescence and using magnetic surface molecularly imprinted particles. Microchim Acta 182:943–948
4. Chen H, Gao F, He R, Cui D (2007) Chemiluminescence of luminol catalyzed by silver nanoparticles. J Colloid Interface Sci 315:158–163
5. Alarfaj NA, Aly FA, El-Tohamy MF (2015) Application of silver nanoparticles to the chemiluminescence determination of cefditoren pivoxil using the luminol-ferricyanide system. Luminescence 30: 91–97
6. Wang L, Tang Y (2011) Determination of dipyridamole using TCPO-H_2O_2 chemiluminescence in the presence of silver nanoparticles. Luminescence 26:703–709
7. Biparva P, Abedirad SM, Kazemi SY (2015) Silver nanoparticles enhanced a novel TCPO-H_2O_2-safraninO chemiluminescence system for determination of 6-mercaptopurine. Spectrochim Acta A 145:454–460
8. Yu X, Jiang Z, Wang Q, Guo Y (2010) Silver nanoparticle-based chemiluminescence enhancement for the determination of norfloxacin. Microchim Acta 171:17–22
9. Wabaidur SM, Alam SM, Alothman ZA, Mohsin K (2015) Silver nanoparticles enhanced flow injection chemiluminescence determination of gatifloxacin in pharmaceutical formulation and spiked urine sample. Spectrochim Acta A 144:170–175
10. Wang J, Park JN, Wei XY, Lee CW (2003) Room-temperature heterogeneous hydroxylation of phenol with hydrogen peroxide over Fe^{2+}, Co^{2+} ion-exchanged Na beta zeolite. Chem Commun 628–629
11. Irons RD (1985) Quinones as toxic metabolites of benzene. J Toxicol Environ Health 16:673–678
12. Keith LH (1991) Comilation of sampling analysis methods. US Environmental Protection Agency, Boca Raton
13. Afkhami A, Khatami HA (2001) Indirect kinetic-spectrophotometric determination of resorcinol, catechol and hydroquinone. J Anal Chem 56:429–432
14. Figueiredo EC, Tarley CRT, Kubota LT, Rath S, Arruda MAZ (2007) On-line molecularly imprinted solid phase extraction for the selective spectrophotometric determination of catechol. Microchem J 85:290–296
15. Lu L, Huang X, Dong Y, Huang Y, Pan X, Wang X, Feng M, Luo Y, Fang D (2015) Facile method for fabrication of self-supporting nanoporous gold electrodes via cyclic voltammetry in ethylene glycol, and their application to the electrooxidative determination of catechol. Microchim Acta 182:1509–1517
16. Han JT, Huang KJ, Li J, Liu YM, Yu M (2012) β-cyclodextrin-cobalt ferrite nanocomposite as enhanced sensing platform for catechol determination. Colloids Surf B: Biointerfaces 98:58–62
17. Zhang H, Huang Y, Hu S, Huang Q, Wei C, Zhang W, Yang W, Dong P, Hao A (2015) Self-assembly of graphitic carbon nitride nanosheets-carbon nanotube composite for electrochemical simultaneous determination of catechol and hydroquinone. Electrochim Acta 176:28–35
18. Liu W, Li C, Tang L, Tong A, Gu Y, Cai R, Zhang L, Zhang Z (2013) Nanopore array derived from l-cysteine oxide/gold hybrids: enhanced sensing platform for hydroquinone and catechol determination. Electrochim Acta 88:15–23
19. Wang Y, Qu J, Li S, Dong Y, Qu J (2015) Simultaneous determination of hydroquinone and catechol using a glassy carbon electrode modified with gold nanoparticles, ZnS/NiS@ZnS quantum dots and L-cysteine. Microchim Acta 182:2277–2283
20. Feng XJ, Shi YL, Hu ZG (2011) Polyaniline/polysulfone composite film electrode for simultaneous determination of hydroquinone and catechol. Mater Chem Phys 131:72–76
21. Lu Q, Hu H, Wu Y, Chen S, Yuan D, Yuan R (2014) An electrogenerated chemiluminescence sensor based on gold nanoparticles@C_{60} hybrid for the determination of phenolic compounds. Biosens Bioelectron 60:325–331
22. Sun YG, Cui H, Li YH, Lin XQ (2000) Determination of some catechol derivatives by a flow injection electrochemiluminescent inhibition method. Talanta 53:661–666
23. Lourenço ELB, Ferreira A, Pinto E, Yonamine M, Farsky SHP (2006) On-fiber derivatization of SPME extracts of phenol, hydroquinone and catechol with GC-MS detection. Chromatographia 63: 175–179
24. Wu YB, Wu JH, Shi ZG, Feng YQ (2009) Simultaneous determination of 5-hydroxyindoles and catechols from urine using polymer monolith microextraction coupled to high-performance liquid chromatography with fluorescence detection. J Chromatogr B 877: 1847–1855
25. Su R, Lin JM, Qu F, Chen Z, Gao Y, Yamada M (2004) Capillary electrophoresis microchip coupled with on-line chemiluminescence detection. Anal Chim Acta 508:11–15
26. Hu Y, Li X, Pang Z (2005) Indirect chemiluminescence detection for capillary zone electrophoresis of monoamines and catechol using luminol-$K_3[Fe(CN)_6]$ system. J Chromatogr A 1091:194–198
27. Xie T, Liu Q, Shi Y, Liu Q (2006) Simultaneous determination of positional isomers of benzenediols by capillary zone electrophoresis with square wave amperometric detection. J Chromatogr A 1109:317–321
28. Li N, Gu J, Cui H (2010) Luminol chemiluminescence induced by silver nanoparticles in the presence of nucleophiles and Cu^{2+}. J Photochem Photobiol A Chem 215:185–190
29. Zhang M, Xiao X, Zeng W, Zeng X, Yao H (2014) Determination of 2-methoxyestradiol in serum samples and pharmaceutical preparations by silver nanoparticles-enhanced chemiluminescence. Talanta 120:331–335
30. Xing L, Tang Y, Wang Z, Song H, Shi X (2013) Sensitive chemiluminescence determination of phentolamine mesylate and phenoxybenzamine hydrochloride based on $K_3Fe(CN)_6$-H_2O_2-fluorescein. J Lumin 137:162–167